The Canadian Mineralogist
Vol. 48, pp. 651-659 (2010)
DOI : 10.3749/canmin.48.3.651

A CRYSTALLOGRAPHIC STUDY OF THE INCOMPLETE SOLID-SOLUTION BETWEEN PLUMBOJAROSITE AND JAROSITE

Laurel C. BASCIANO and Ronald C. PETERSON§

Department of Geological Sciences and Geological Engineering, Queen's University, Kingston, Ontario K7L 3N6, Canada

Abstract

An incomplete solid-solution series exists between jarosite, $KFe_3(SO_4)_2(OH)_6$, and plumbojarosite, $Pb[Fe_3(SO_4)_2(OH)_6]_2$, on the basis of experimental data and the observed chemical variations of these minerals in nature. Samples were synthesized in a chloride-rich solution at 140° and 110°C and studied using X-ray powder diffraction, Rietveld analysis and chemical analysis. Under these conditions, plumbojarosite will only precipitate if the solution has a high concentration of Pb, 99 mol.% Pb. Only jarosite forms from solutions with up to 79 mol.% Pb in the starting solution. At 85 mol.% Pb in the solution, both jarosite and plumbojarosite precipitate. At the conditions of synthesis, Pb substitution into jarosite is extremely limited, with occupancy of 2% in the potassium site. Increased Pb in the starting solution resulted in no increased substitution of Pb into jarosite, but an increased substitution of H_3O^+ into the structure. An increase in charge due to Pb^{2+} substitution at the *A* site causes a charge imbalance in the structure. Potassium substitution into plumbojarosite is more extensive, K/(Pb + K) = 32%. Potassium substitution preferentially occurs in one of the two symmetrically distinct *A*-sites, based on a Rietveld refinement of site populations.

Keywords: jarosite, plumbojarosite, sulfate mineralogy, environmental mineralogy, crystal structure, powder diffraction, Rietveld analysis.

Sommaire

Une solution solide incomplète existe entre la jarosite, $KFe_3(SO_4)_2(OH)_6$, et la plumbojarosite, $Pb[Fe_3(SO_4)_2(OH)_6]_2$, jugeant des données expérimentales et des variations en composition observées dans ces minéraux dans la nature. Nous avons synthétisé certaines compositions de la série à partir de solutions chlorurées à 140° et 110°C, et nous les avons caractérisé au moyen de diffraction X sur poudres, analyse de Rietveld, et analyse chimique. A ces conditions, la plumbojarosite ne peut précipiter que si la solution possède une forte concentration de Pb, 99% sur une base molaire. Seule la jarosite cristallise à partir de solutions ayant jusqu'à 79% de Pb au départ. A un niveau de 85% Pb en solution, jarosite et plumbojarosite se forment ensemble. Aux conditions de synthèse, l'incorporation du Pb dans la jarosite est fortement limité, avec un taux d'occupation de 2% au site du potassium. Une augmentation dans la teneur en Pb de la solution de départ n'a pas mené à une augmentation du taux de substitution du Pb dans la jarosite, mais nous documentons une augmentation dans la substitution de H_3O^+ dans la structure. Une augmentation de charges due à l'incorporation du Pb^{2+} au site *A* mène à une distribution de charges non balancée dans la structure. Par contre, plus de potassium pent être accommodé dans la plumbojarosite, jusqu'à K/(Pb + K) = 32%. Le potassium semble préférer un des deux sites *A* symétriquement distincts, selon les résultats de l'affinement Rietveld de la population des sites.

(Traduit par la Rédaction)

Mots-clés: jarosite, plumbojarosite, minéralogie des sulfates, minéralogie environnementale, structure cristalline, diffraction sur poudres, analyse Rietveld.

Introduction

Plumbojarosite, $Pb[Fe_3(SO_4)_2(OH)_6]_2$, is a supergene mineral primarily found in gossans, which overlie massive sulfide deposits. Gossans are the residues of an intense acidic leaching, and are commonly enriched in trace elements such as Au, Ag, As and Pb with respect to the original sulfide. Gossan deposits are important because of their ability to fix toxic elements such as Pb and As (Nieto *et al.* 2003) as well as concentrating metals of economic importance. Plumbojarosite is commonly found closely associated with jarosite, $KFe_3(SO_4)_2(OH)_6$, in gossan deposits and in acid mine-waste where lead is available for uptake (De Oliveira *et al.* 1996).

---

§ *E-mail address*: peterson@geol.queensu.ca

The purpose of the study was to determine at what point in the solid-solution series the unit cell doubles to accommodate Pb^{2+} into the structure on the basis of natural and synthetic samples. Plumbojarosite and jarosite are members of the jarosite group, which is part of the alunite supergroup (Jambor 1999). Jarosite-group minerals have a rhombohedral symmetry, space group $R\overline{3}m$, with hexagonal cell-parameters a ~7.3 Å, c ~17 Å. The alunite supergroup consists of over 40 different mineral species with the general formula $AB_3(TO_4)_2(OH)_6$. There is extensive solid-solution involving the A, B and T sites within the alunite supergroup, where A may contain H_3O^+, Na^+, K^+, Rb^+, Ag^+, Tl^+, NH_4^+, ½ Ca^{2+} or ½ Pb^{2+}, B is Fe^{3+} or Al^{3+}, and TO_4 is SO_4^{2-}, PO_4^{3-} or AsO_4^{3-} (Scott 1987, Stoffregen & Alpers 1987). The jarosite group is characterized by $B = Fe^{3+}$ and T = S. Jarosite (A = potassium) and natrojarosite (A = sodium) are the most prevalent naturally occurring jarosite-group minerals. There is a common substitution of hydronium at the A cation site in synthetic jarosite-group phases (Basciano & Peterson 2007, 2008).

Plumbojarosite was first described in 1902 as a mineral species related to jarosite with a lead-rich composition (Hildebrand & Wright 1910). Plumbojarosite has been recognized as an economically important mineral, as Ag commonly substitutes in its structure during the alteration of the original sulfide ore. The Pb and Ag content of plumbojarosite is high enough that it is a profitable source of both Pb and Ag. This fact was addressed in Dutrizac & Jambor (1983, 1987), Szymański (1985), Amorós *et al.* (1981), Roca *et al.* (1999) and Frost *et al.* (2005). The plumbojarosite structure was solved by Szymański (1985) with a sample from the Tintic Standard mine, Dividend, Utah, USA. Its unit-cell parameter c is doubled, compared to jarosite, as a result of the order of Pb^{2+} and a vacancy replacing $2K^+$ in the structure. The chemical formula is expressed as $Pb_{0.5}\square_{0.5}Fe_3(SO_4)_2(OH)_6$ or, simplified, $Pb_{0.5}Fe_3(SO_4)_2(OH)_6$. The doubling results in two crystallographically distinct A-site positions. The crystal structure showing the two A-sites is shown in Figure 1.

Three natural samples were analyzed in addition to the samples synthesized for this study. The three natural samples were supplied by CANMET, Natural Resources Canada, Ottawa, Canada. The first sample is from the Apex mine in Washington County, Utah. The second sample is from Chihuahua, Mexico, and the third is from the Rube mine, Gold Hill, Utah. The jarosite – plumbojarosite solid-solution series was also investigated using synthetic samples of various compositions. Unexpectedly, very little substitution of Pb^{2+} into the

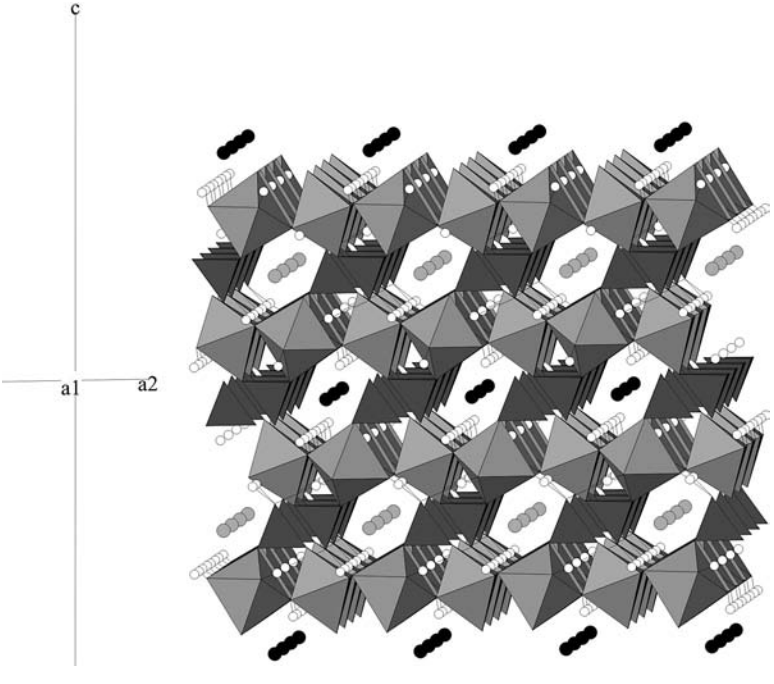

FIG. 1. The crystal structure of plumbojarosite showing the $A2$ (dark) and $A1$ (light) atomic sites alternating along the c axis (view along the a axis). Sulfate tetrahedra and iron-containing octahedra are shown as filled and shaded polyhedra, and the hydrogen atoms, as unfilled circles.

TABLE 1. CHEMICAL COMPOSITIONS OF STARTING SOLUTIONS AND RESULTING SOLID COMPOSITIONS

Starting solution composition (g)	K_2SO_4	0.5	0.4	0.25	0.2	0.15	0.08	0.02	0.0
	$PbSO_4$	0.0	0.1	0.25	0.3	0.35	0.42	0.48	0.5
Mol.% Pb		0	48	79	85	90	95	99	100
Sample name	140°C	**A**	**B**	**C**	**D**	**E**	**F**	**G**	**H**
		Jrs	Jrs	Jrs, $PbCl_2$	Jrs, Pjr	Jrs, Pjr	Jrs, Pjr, $PbSO_4$	Pjr	Pjr, $PbCl_2$
Sample name	110°C	-	**I**	**J**	-	**K**	**L**	**M**	-
		-	Jrs	Jrs, $PbCl_2$	-	Jrs, Pjr, $PbSO_4$	Jrs, Pjr, $PbSO_4$	Pjr	-

Note: Jrs: jarosite, Pjr: plumbojarosite. The conditions of synthesis are described in the text.

structure of jarosite was observed at the temperatures studied. Samples were characterized with powder X-ray diffraction, Rietveld refinement and chemical analysis.

SYNTHESIS OF MEMBERS OF THE SERIES

Samples were synthesized in a chloride-rich medium using a method similar to that described by Frost *et al.* (2005). A similar method was also used by Dutrizac (1991). The high concentration of chloride eliminates the precipitation of $PbSO_4$. Five mL of 1.23 M $FeCl_3$ solution and a mixture of KCl and $PbCl_2$ totaling 0.5 grams (see Table 1 for ratio) were dissolved in 12 mL of concentrated LiCl solution. Six grams of $Fe(SO_4)_3$•$5H_2O$ were dissolved in 25 mL of deionized water and added to the chloride solution. Two sets of each starting solution were mixed, and each was heated for 48 hours in a stainless steel pressure bomb at 140°C or 110°C. The starting solutions, conditions of synthesis and resulting solid phases are shown in Table 1. The resulting powders are yellow and fine-grained, and are either jarosite, plumbojarosite or a mixture of jarosite and plumbojarosite. Several final samples were found to contain $PbCl_2$ or $PbSO_4$. All of the samples were rinsed thoroughly with deionized water to remove $PbCl_2$ before chemical analysis and data collection for Rietveld refinement. The $PbSO_4$ has much lower solubility than $PbCl_2$ and remained in the samples after washing. The samples were filtered and then dried at 110°C.

In two previous studies of jarosite-group minerals (Basciano & Peterson 2007, 2008), we found that there was peak broadening due to non-homogeneity of the samples synthesized. The broadening is most evident in peaks where there is a large difference in peak position between end-member phases in the mixture (*e.g., hkl* = 006). When these samples are ground and reheated in the reactant solution, the samples become homogeneous. We initially considered that the same behavior would occur in the current study for samples that contain both jarosite and plumbojarosite. However, we found no peak broadening, only distinct peaks attributable to either jarosite or plumbojarosite. To ensure that the solid is in equilibrium with the solution, one sample was reheated in the original solution for 12 days at 140°C and analyzed with X-ray diffraction every three days to determine if any peak shifts occurred. The peak positions and peak widths remained the same after 12 days of annealing.

X-RAY POWDER DIFFRACTION AND RIETVELD ANALYSIS

Powder-diffraction data were collected from 5° to 100° 2θ (Fe filtered Co*K*α radiation) from a back-packed sample using a Panalytical X'Pert theta–theta diffractometer and an X'celerator position-sensitive detector equipped with incident- and diffracted-beam soller slits, and ½° divergence and 1° anti-scatter slits. The normal-focus Co X-ray tube was operated at 40 kV and 45 mA. Profiles were taken with an effective step-interval of 0.008° 2θ, and counting time per step of 40 seconds. Data were refined with the Rietveld refinement program "Topas Academic" (Coelho 2004). Starting atomic parameters for jarosite and plumbojarosite were taken from Basciano & Peterson (2007) and Szymański (1985), respectively. The instrument parameters were modeled using a full axial divergence model defined by Cheary & Coelho (1998). The Co*K*α source-emission profiles were taken from Hölzer *et al.* (1997). The hydrogen positions (OH group) in jarosite samples were taken from the single-crystal study of hydroniumjarosite by Majzlan *et al.* (2004). Unit-cell parameters were refined for all samples except for sample G, for which the atom positions, displacement parameters and site occupancies also were refined. Hydrogen-bond lengths were restrained to be 0.78 Å during the refinement. Displacement parameters of the oxygen atoms were constrained to be equal, and the displacement parameters of H were set to $U_{iso} = 0.025$ and not refined. Final refinement of sample G gave the following agreement-factors: $R_p = 4.975$, $R_{wp} = 6.759$, $R_{exp} = 4.080$ and Goodness of Fit (Young 1993) = 1.656. We included $PbSO_4$ in the model where needed to account for any $PbSO_4$ that precipitated from solution during the synthesis.

The X-ray-diffraction patterns for jarosite and plumbojarosite are very similar and can be difficult to distinguish without high-quality data. Plumbojarosite does have an additional weak reflection at d = 11.25 Å owing to the doubled c axis. Where the sample consists of jarosite and plumbojarosite, subtle widening or doubling of peaks due to the differences in unit-cell dimensions can be noted.

CHEMICAL ANALYSIS

The iron, lead, potassium and sulfur content of the solid samples containing either jarosite or plumbojarosite were determined using a Varian Vista CCD Simultaneous ICP–OES at Analytical Services Unit, Queen's University. The samples were digested in *aqua regia* and diluted for analysis. The average analytical accuracy and precision for each element are: Fe ± 2%, 4.1%; Pb ± 3%, 4.9%; K ± 5%, 4.7% and S ± 2%, 5.3%. From these data, the stoichiometry of the alkali and iron sites was determined in the solid samples on the basis of the ratio of alkali and iron to sulfur. The atomic percentages of potassium, lead and iron in these sites were normalized to two sulfur atoms per formula unit. The chemical compositions of synthetic samples are given in Table 2. The Fe^{3+} is equal to three atoms per formula unit within error, and we assume that this site is fully occupied by ferric iron for charge-balance considerations. Samples containing both jarosite and plumbojarosite or those containing $PbSO_4$ were not chemically analyzed as potassium and lead content could not be accurately attributed to jarosite or plumbojarosite. The H_3O content was obtained by assuming charge balance, full occupancy by Fe^{3+}, and no H_2O-for-OH^- substitution.

TABLE 2. CHEMICAL COMPOSITION[§] OF SYNTHETIC JAROSITE AND PLUMBOJAROSITE

Sample	Formula
A*	$K_{0.95}\,(H_3O)_{0.05}\,Fe_{2.87}\,(SO_4)_2\,(OH)_6$
B	$K_{0.99}\,(H_3O)_{0.01}\,Fe_{2.96}\,(SO_4)_2\,(OH)_6$
C	$K_{0.91}\,Pb_{0.02}\,(H_3O)_{0.05}\,Fe_{2.95}\,(SO_4)_2\,(OH)_6$
G	$Pb_{0.34}\,K_{0.16}\,(H_3O)_{0.16}\,Fe_{2.95}\,(SO_4)_2\,(OH)_6$
H	$Pb_{0.33}\,(H_3O)_{0.34}\,Fe_{3.01}\,(SO_4)_2\,(OH)_6$
I	$K_{0.99}\,(H_3O)_{0.01}\,Fe_{2.97}\,(SO_4)_2\,(OH)_6$
J	$K_{0.92}\,Pb_{0.01}\,(H_3O)_{0.06}\,Fe_{3.08}\,(SO_4)_2\,(OH)_6$
M	$Pb_{0.32}\,K_{0.13}\,(H_3O)_{0.23}\,Fe_{3.00}\,(SO_4)_2\,(OH)_6$

* Data taken from Basciano & Peterson (2007).

[§] Analytical results (ICP–OES).

RESULTS

Synthesis

Jarosite or plumbojarosite precipitated in the synthesis experiments with no complete solid-solution between end members at the temperatures of synthesis selected (110° and 140°C). Synthesis conditions and the resulting solids are listed in Table 1. The starting solution must contain a high concentration of $PbSO_4$ and very little K_2SO_4 for plumbojarosite to form without forming jarosite. Only jarosite crystallized from solutions with 0, 48 and 79 mol.% Pb. Jarosite and plumbojarosite precipitated from the solutions with 85 and 95 mol.% Pb. Only plumbojarosite crystallized in the solution containing 99 mol.% Pb.

In samples containing both jarosite and plumbojarosite, only a finite amount of lead can be taken from solution by the plumbojarosite as there is limited incorporation of Pb in the structure of jarosite. The remaining lead in solution precipitates as $PbSO_4$ or $PbCl_2$. At 79 mol.% Pb, $PbCl_2$ crystallized out of solution as large white crystals with jarosite. As we increased the mol.% Pb in the solution, $PbSO_4$ precipitated with the jarosite–plumbojarosite mixture. At 99 mol.% Pb, plumbojarosite precipitated with no $PbSO_4$. It is evident that at this concentration, a sufficient amount of Pb is removed from solution by plumbojarosite to prevent the precipitation of $PbSO_4$. If the mol.% Pb in solution is increased to 100%, plumbojarosite and minor $PbCl_2$ precipitate.

ATOMIC SUBSTITUTIONS IN JAROSITE AND PLUMBOJAROSITE

Refined unit-cell parameters for jarosite and plumbojarosite are given in Table 3. The variation of these parameters with the concentration of Pb in the synthesis solution is presented in Figure 2. In Figure 2a, the c parameter of plumbojarosite decreases as the concentration of Pb in the synthesis solution increases. The lowest value of c is obtained for plumbojarosite grown in the solution with the highest concentration of Pb in solution. The plumbojarosite grown at 110°C has a significantly shorter c parameter (33.706 Å) than that grown at 140°C (33.7274 Å), even though they were synthesized from solutions with the same concentration of Pb and K. At the temperatures and conditions of synthesis, there is limited Pb substitution in jarosite. Chemical analysis reveals that there is no Pb or H_3O substitution in samples B or I, and these samples are close to the end-member composition of jarosite. The A-site occupancy of sample C is 91% K, 2% Pb based on chemical analysis, and 5% H_3O^+ is assumed to maintain charge balance. These samples have the largest c dimensions of the samples studied. The A-site occupancy of sample J is similar to that of sample C (Fig. 2b). Unit-cell refine-

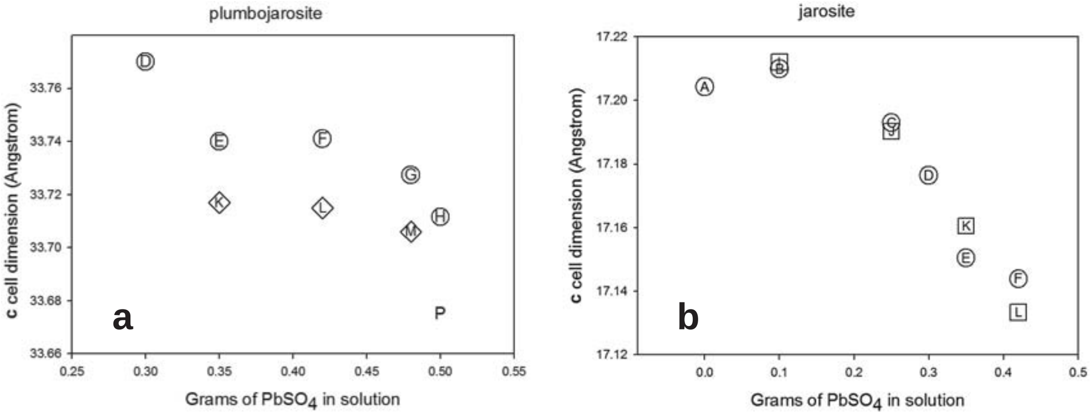

FIG. 2. Variation in cell dimensions of synthetic plumbojarosite (a) and jarosite (b) as a function of the Pb content of the starting solution. Synthesis runs at 140°C are plotted as circles, 110°C runs as squares. The natural sample studied by Szymański (1985) is shown as P.

TABLE 3. UNIT-CELL PARAMETERS OF SYNTHETIC SAMPLES, DETERMINED BY RIETVELD REFINEMENT

Sample		a (Å)	c (Å)	Temperature of synthesis
Plumbojarosite Szymański (1985)		7.3055(7)	33.675(2)	Natural
A*	jarosite	7.30293(8)	17.2043(2)	140°C
B	jarosite	7.3072(1)	17.2099(3)	140°C
C	jarosite	7.3089(1)	17.1930(3)	140°C
D	jarosite	7.3110(2)	17.1764(4)	140°C
D	plumbojarosite	7.3173(5)	33.770(2)	140°C
E	plumbojarosite	7.3151(2)	17.1504(6)	140°C
E	plumbojarosite	7.3160(2)	33.740(1)	140°C
F	jarosite	7.3156(3)	17.1439(8)	140°C
F	plumbojarosite	7.3168(2)	33.741(1)	140°C
G	plumbojarosite	7.3185(2)	33.7274(8)	140°C
H	plumbojarosite	7.3199(2)	33.7116(8)	140°C
I	jarosite	7.3046(1)	17.2120(3)	110°C
J	jarosite	7.3107(1)	17.1902(3)	110°C
K	jarosite	7.3142(2)	17.1605(5)	110°C
K	plumbojarosite	7.3166(2)	33.717(1)	110°C
L	jarosite	7.3174(2)	17.1333(7)	110°C
L	plumbojarosite	7.3190(2)	33.715(1)	110°C
M	plumbojarosite	7.3186(2)	33.706(1)	110°C

* Data from Basciano & Peterson (2007).

ment of the jarosite in samples D, E and F shows that *c* decreases with an increase in the amount of Pb available in the synthesis solution (Fig. 2b). The decrease in the cell parameter *c* is assumed to be caused by substitution of H_3O^+ for K^+. The jarosite in samples C and J also show a slight decrease in *c*. Details of the jarosite – hydroniumjarosite solid-solution series can be found in Basciano & Peterson (2007).

Potassium substitution in plumbojarosite is more extensive than lead substitution in jarosite. The total occupancy of the *A* sites in end-member plumbojarosite (sample H) is 33% Pb, as determined by ICP–OES. If charge balance is assumed and no H_2O-for-OH^- substitution exists, then the total *A*-site occupancy must involve 34% H_3O^+. The site occupancy of samples G and M is similar; G: 34% Pb^{2+}, 16% K^+ and 16% H_3O^+ and M: 32% Pb^{2+}, 13% K^+ and 23% H_3O^+. As chemical analysis cannot be done on the samples that contain both jarosite and plumbojarosite, we assume that the plumbojarosite in these samples contains K^+ at the *A* site as well as H_3O^+. This is based on the observation that plumbojarosite samples G and M contain K^+.

At 140°C, there is a progressive decrease in the *c* parameter of jarosite and plumbojarosite with increasing Pb content and decreasing K in the starting solution. As the Pb content of the starting solution increases, the cell parameter *c* of jarosite decreases owing to increasing H_3O^+ at the *A* site (Fig. 2b). This decrease continues in jarosite precipitated from solutions with increased Pb content, where plumbojarosite begins to precipitate as well. The cell parameter *c* of plumbojarosite decreases with increasing Pb concentration and decreasing K concentration in the starting solution (Fig. 2a). This increase is caused by Pb substitution at the *A* site.

At 110°C, there is a similar trend. With increasing hydronium substitution in jarosite, the cell parameter *c* decreases. At 110°C, there is little change in the parameters in plumbojarosite with increased K in the starting solution, and the *c* dimensions are significantly lower than those of the plumbojarosite grown at 140°C. From this, we conclude that at 110°C, less substitution of K for Pb occurs in plumbojarosite.

The unit-cell parameters of three natural samples of plumbojarosite were determined to compare with the synthetic product (Fig. 3). These parameters were determined on the fine yellow powders using Rietveld refinement, and the chemical analyses were done by CANMET, Natural Resources Canada, Ottawa, Canada. The natural samples from the Apex mine, Washington County, Utah and the Rube mine, Gold Hill, Utah, show minor impurities and cell parameters close to our sample G. The bulk composition of the Apex mine sample is 14.0% Pb, 0.46% K, 0.16% Na, 26.23% Fe and 25.5% SO_4. The bulk composition of the Rube mine sample is 17.48% Pb, 0.21% K, 0.30% Na, 0.29% Ag, 27.34% Fe, 0.10% Al and 26.17% SO_4. The sample from Chihuahua, Mexico has a bulk composition of 13.7% Pb, 2.00% K, 0.08% Na, 22.63% Fe and 22.32% SO_4. The sample from Chihuahua contains minor admixed gypsum and quartz, which were included in the Rietveld analysis. Owing to the high acid-insoluble content of the sample, the results are low for Fe and SO_4. The higher K content of this sample is reflected in the unit-cell parameters. The *c* parameter for the sample from Chihuahua is larger than that of the samples synthesized in this study. There may be a small component of jarosite admixed in the sample, on the basis of the excess of potassium measured during chemical analysis, although there are no obvious peaks that can unquestionably be attributed to jarosite. As the cell parameters of the plumbojarosite are shifted, and there is a similarity of the plumbojarosite pattern to the jarosite pattern, jarosite could not be reliably added to the refinement. The increased amount of K^+ substitution in this natural sample over that achieved in the synthetic study is probably due to the different temperature and slower conditions of growth experienced by the natural sample.

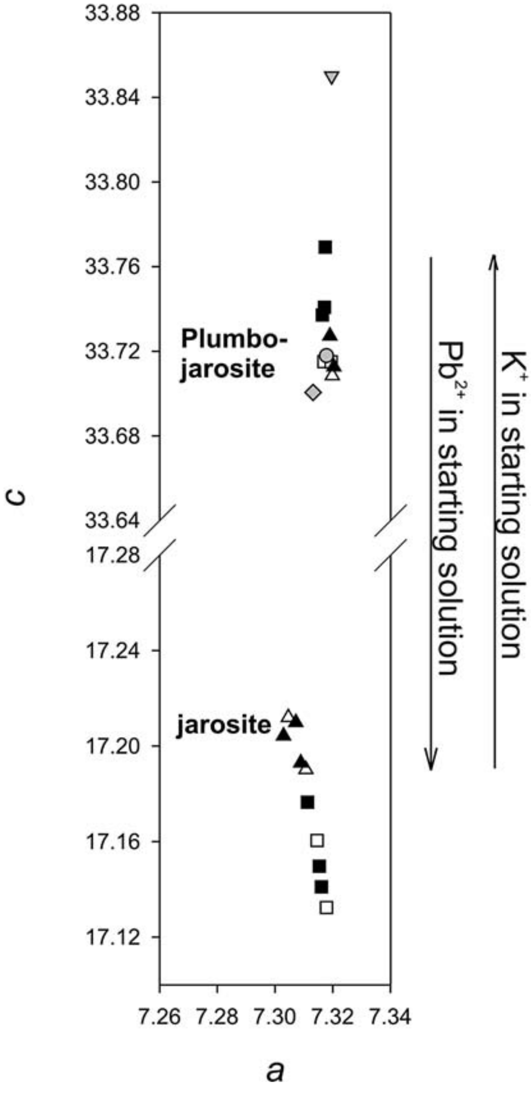

FIG. 3. Variation in cell dimensions for all synthetic and natural samples that were studied. Symbols: ■ samples with jarosite or plumbojarosite (140°C), △ samples with jarosite and plumbojarosite (140°C), □ samples with jarosite or plumbojarosite (110°C), ▲ samples with jarosite and plumbojarosite (110°C), ● plumbojarosite from the Rube mine, Utah, ◇ plumbojarosite from the Apex mine, Utah, ▽, sample of plumbojarosite from Chihuahua, Mexico.

Crystal chemistry of K and H_3O substitution in plumbojarosite

The crystal structure of sample G (plumbojarosite with 34% potassium total *A*-site occupancy, as determined by ICP–OES) was refined using X-ray powder diffraction and Rietveld refinement. The results are presented in Tables 4 and 5. Sample G was chosen because it is a single phase for which a chemical

TABLE 4. RIETVELD-REFINED ATOM POSITIONS, ISOTROPIC DISPLACEMENT PARAMETERS AND OCCUPANCIES OF SYNTHETIC SAMPLE G

Site		*x*	*y*	*z*	U_{iso}	N
*A*1(Pb)	3*b*	0	0	0	0.010(6)	0.130(4)
*A*1(K)	3*b*	0	0	0	0.010(6)	0.371(4)
S1	6*c*	0	0	0.1549(3)	0.006(6)	1
O1	6*c*	0	0	0.1987(5)	0.027(1)	1
O2	18*h*	0.2182(6)	2*x*	0.0270(3)	0.027(1)	1
O3	18*h*	0.1226(6)	2*x*	-0.0725(2)	0.027(1)	1
H1	18*h*	0.141(3)	2*x*	-0.051(1)	0.025	1
*A*2(Pb)	3*a*	0	0	0.5	0.039(2)	0.547(4)
S2	6*c*	0	0	0.6546(2)	0.041(6)	1
O4	6*c*	0	0	0.6981(3)	0.027(1)	1
O5	18*h*	0.2212(6)	2*x*	0.5258(3)	0.027(1)	1
O6	18*h*	0.1312(6)	2*x*	0.4355(3)	0.027(1)	1
H2	18*h*	0.189(3)	2*x*	0.444(1)	0.025	1
Fe	18*h*	0.1677(4)	2x	0.0830(2)	0.022(1)	1

Note: Numbers in parentheses in this and subsequent tables are estimated standard deviations. N: occupancy.

analysis was done, and there is K^+-for-Pb^{2+} substitution. Charge balance may be achieved by substitution of H_3O^+ at the *A* site or protonation of OH^- to form H_2O, as was proposed by Kubisz (1970) and Wills & Harrison (1996) for alunite-group structures where there is a cation deficiency at the B^{3+} site.

To determine if there is any order at sites *A*1 (0, 0, 0) and *A*2 (0, 0, 0.5), the occupancies of these sites were refined but were not constrained to the chemical data and the requirement of full site-occupancy. Atoms Pb1, Pb2, K1 and K2 were refined independently. The site occupancies of Pb and K at the *A*1 site refined to 0.130(4) and 0.371(4), respectively. The site occupancy of Pb at the *A*2 site refined to 0.547(4), and the occupancy of K at the *A*2 site refined to zero, within error. Total Pb at the combined *A*-site refines to 0.338, and the K occupancy refines to 0.186. These values are very close to *A*-site occupancies measured with ICP–OES, which are 34% Pb and 16% K. From these results, we conclude that there is cation order at the *A* sites. The majority of the lead is located at *A*2, with much less lead at *A*1, and all of the potassium is located at *A*1.

The refined structure of sample G is very similar to that of plumbojarosite as determined by Szymański (1985). The occupancies were determined to be 0.039 and 0.0961 for Pb1 and Pb2 in that natural sample. In the current study, the *A*1 polyhedron, which contains Pb and K with the remainder vacant, has bond lengths of 2.896(8) and 2.913(8) Å. The *A*2 polyhedron, which is partially occupied by Pb and partially vacant, has bond lengths of 2.738(9) and 2.936(5) Å. We expect that the site that contains potassium has longer bond-lengths, as K^+ has a larger ionic radius than Pb^{2+}, 1.38 Å and 1.19 Å, respectively (Shannon 1976). Both sites have some level of vacancy, which leads to longer bond-lengths overall (Shannon 1976). The *A*1 polyhedron has marginally shorter bond-lengths than those found by Szymański (1985) owing to the higher occupancy of this different material. In the plumbojarosite structure determined by Szymański (1985), the *A*1 site is close to being vacant, whereas *A*2 has close to full occupancy by Pb. The *A*2 site of sample G has slightly longer bonds owing to partial occupancy.

TABLE 5. SELECTED INTERATOMIC DISTANCES (Å) AND ANGLES (°) OF SAMPLE G AS DETERMINED BY RIETVELD REFINEMENT OF POWDER X-RAY-DIFFRACTION DATA

*A*1* – O3 × 6	2.896(8)	*A*2 – O6 × 6	2.738(9)
*A*1* – O2 × 6	2.913(8)	*A*2 – O5 × 6	2.936(5)
Average	2.904		2.837
S1 – O1	1.47(2)	S2 – O4	1.47(1)
S1 – O5 × 3	1.498(9)	S2 – O2 × 3	1.543(9)
Average	1.491	Average	1.524
O1 – S1 – O5 × 3	108.4(3)	O4 – S2 – O2 × 3	109.1(5)
O5 – S1 – O5 × 3	110.5(5)	O2 – S2 – O2 × 3	109.9(5)
Average	109.4	Average	109.5
Fe – O3 × 2	1.938(5)	O3 – H1#	0.75(5)
Fe – O2	1.99(1)	O3 – H1 ··· O4	2.528(2)
Fe – O6 × 2	2.025(4)		
Fe – O5	2.07(1)	O6 – H2#	0.79(4)
Average	2.00	O6 – H2 ··· O3	2.69(3)

* *A*1 = Pb and K, # restrained.

The Fe atom is octahedrally coordinated with four hydroxyl groups around the equatorial plane and two oxygen atoms in the axial positions. The Fe–O bonds are slightly shorter than those found by Szymański (1985), as there is partial occupancy of both *A*1 and *A*2 sites and K^+-for-Pb^{2+} at the *A*1 site. The lengthening in the *A*1–O and *A*2–O bond lengths is correlated with a shortening in the Fe–O bond lengths.

Substitution of H_3O and K in plumbojarosite causes an increase in unit-cell parameters *a* and *c*. The difference is more pronounced in the *c* direction, as is the case with substitution at the *A* site of other jarosite-group members (Basciano & Peterson 2007).

DISCUSSION

From chemical analysis and Rietveld refinement, we found that at the conditions of synthesis, there is essentially no substitution of Pb^{2+} for K^+ in the jarosite structure, but a substitution of H_3O^+ instead. Previous investigators (Basciano & Peterson 2007, Nielson *et al.* 2007, Majzlan *et al.* 2004, Drouet & Natrotsky 2003, Ripmeester *et al.* 1986) found extensive substitution of H_3O^+ for K^+ in jarosite. As K decreases in the starting solution and Pb^{2+} increases, there is less K^+ available for substitution, and H_3O^+ substitution occurs, as found by Basciano & Peterson (2007). Potassium is preferentially taken into the jarosite structure owing to the marked difference in solubility of jarosite over hydroniumjarosite. End-member solubility products from PHREEQC (Parkhurst & Appelo 2000) are: $10^{-5.39}$ for hydroniumjarosite and $10^{-9.21}$ for jarosite. Substitution of Pb^{2+} for K^+ is extremely limited in jarosite owing to the difference in charge and size.

In contrast, there is extensive substitution of K^+ and H_3O^+ for Pb^{2+} in the plumbojarosite structure. The plumbojarosite synthesized in this study (sample H) has 33% Pb^{2+} occupancy at the *A* sites, as determined by chemical analysis. In samples G and M, where there was very little potassium added to the starting solution, the plumbojarosite has substantial K incorporated at the *A* site. As is the case of jarosite, potassium is preferentially taken into the structure over hydronium (Basciano & Peterson 2007). Substitution of K^+ and H_3O^+ into the plumbojarosite structure may be charge-balanced in a number of ways. It may be maintained by protonation of OH^- to form H_2O, as was proposed by Kubisz (1970) and Wills & Harrison (1996) to compensate for deficiencies at the *B* site in jarosite- and alunite-group structures. Nielson *et al.* (2007) postulated that vacancies at the *B* site are compensated by the addition of 4 H^+

ions, resulting in four Al–$\mathrm{OH_2}$ bonds per vacancy. This substitution would be accompanied by deprotonation of $\mathrm{H_3O^+}$ at the *A* site, forming $\mathrm{H_2O}$, which is then unnecessary for charge balance, resulting in an *A*-site vacancy.

Other structures in the alunite supergroup that incorporate $\mathrm{Pb^{2+}}$ at the *A* site without doubling of the unit cell must compensate for the charge discrepancy differently. In beudantite, $\mathrm{PbFe_3(SO_4)(AsO_4)(OH)_6}$, which is part of the crandallite group (Jambor 1999), the additional $\mathrm{Pb^{2+}}$ ions per formula unit are compensated by the replacement of 50% of the $\mathrm{SO_4}$ groups by $\mathrm{AsO_4}$ groups. There is limited solubility of As in jarosite (Savage *et al.* 2005), but there is a complete solid-solution between jarosite and beudantite (Scott 1987). There is a progressive substitution of trivalent for divalent anions in $T\mathrm{O_4}$, which is accompanied by a concurrent change from monovalent to divalent cations at the *A* sites. This progression most likely continues to form segnitite, $\mathrm{PbFe_3H(AsO_4)_2(OH)_6}$.

Evidence of an incomplete solid-solution between jarosite and plumbojarosite is apparent in previous studies done on natural samples. Szymański (1985), who solved the structure of plumbojarosite using a natural sample, noted that the single crystal used for the study has a rim of plumbojarosite and a thin core of jarosite. The core has minor $\mathrm{Pb^{2+}}$ substitution (wt%: 7.0 K, 1.2 Pb, 32.7 Fe and 12.9 S), and the rim of plumbojarosite shows no K substitution (wt%: 0.0 K, 18.4 Pb, 29.5 Fe and 11.7 S). He noted in that study that Jambor & Dutrizac (1983) examined many samples from the same locality (Tintic Standard mine, Dividend, USA) and found that the majority show compositional zoning (jarosite core with a plumbojarosite rim).

In many cases, natural samples from gossans related to the Pb–Zn mineralization in the Canoas district, Brazil, are distinctly zoned with close to end-member jarosite or plumbojarosite (De Oliveira *et al.* 1996). Several samples have mid-point composition between jarosite and plumbojarosite, and probably have the plumbojarosite structure with potassium substitution at the *A* site. None of the samples were examined in detail with X-ray diffraction, however.

From this study and previous ones, we contend that there is limited $\mathrm{Pb^{2+}}$ solubility in the jarosite structure. There is extensive solubility of monovalent cations in the plumbojarosite structure, and charge balance is maintained by incorporating $\mathrm{H_3O^+}$and site vacancies.

ACKNOWLEDGEMENTS

The authors thank John Dutrizac, CANMET, Natural Resources Canada, Ottawa, Canada for the natural samples and chemical analysis of these samples. We thank Queen's University Analytical Services Unit for chemical analysis of the synthetic samples. The manuscript was greatly improved with comments from reviewers U. Kolitsch and I. Grey, Associate Editor Peter Leverett and Editor Robert F. Martin. The research was funded by NSERC and OGS grants to L.C.B. and an NSERC Discovery Grant to R.C.P.

REFERENCES

AMORÓS, J.L., LUNAR, R. & TAVIRA, P. (1981): Jarosite: a silver-bearing mineral of the gossan of Rio Tinto (Huelva) and La Union (Cartagena, Spain). *Mineral. Deposita* **16**, 205-213.

BASCIANO, L.C. & PETERSON, R.C. (2007): Jarosite – hydronium jarosite solid-solution series with full iron site occupancy: mineralogy and crystal chemistry. *Am. Mineral.* **92**, 1464-1473.

BASCIANO, L.C. & PETERSON, R.C. (2008): Crystal chemistry of the natrojarosite – jarosite and natrojarosite – hydronium jarosite solid solution series: a synthetic study with full iron site occupancy. *Am. Mineral.* **93**, 853-862.

CHEARY, R.W. & COELHO, A.A. (1998): Axial divergence in a conventional X-ray powder diffractometer. I. Theoretical foundations. *J. Appl. Crystallogr.* **31**, 851-861.

COELHO, A.A. (2004): *TOPAS – Academic*. www.topas-academic.net

DE OLIVEIRA, S.M.B., BLOT, A., IMBERNON, R.A.L. & MAGAT, P. (1996): Jarosita e plumbojarosite nos gossans do districto mineiro de Canoas (PR). *Rev. Brasil. Geociências* **26**, 3-12.

DROUET, C. & NAVROTSKY, A. (2003): Synthesis, characterization and thermochemistry of K–Na–$\mathrm{H_3O}$ jarosites. *Geochim. Cosmochim. Acta* **67**, 2063-2076.

DUTRIZAC, J.E. (1991): The precipitation of lead jarosite from chloride media. *Hydrometallurgy* **26**, 327-346.

DUTRIZAC, J.E. & JAMBOR, J.L. (1983): Formation and characterization of argentojarosite and plumbojarosite and their relevance to metallurgical processing. *Proc. ICAM '84 (Los Angeles)*.

DUTRIZAC, J.E. & JAMBOR, J.L. (1987): The behavior of silver during jarosite precipitation. *Trans. Inst. Mining Metall. C. Mineral Processing and Extractive Metallurgy* **96**, C206-C218.

FROST, R.L., WILLS, R.A., WEIR, M.L., MUSUMECI, A.W. & MARTENS, W. (2005): Thermal decomposition of natural and synthetic plumbojarosites: importance in "archeochemistry". *Thermochim. Acta* **432**, 30-35.

HILLEBRAND, W.F. & WRIGHT, F.E. (1910): A new occurrence of plumbojarosite. *Am. J. Sci.* **180**, 191-192.

HÖLZER, G., FRITSCH, M., DEUTSCH, M., HÄRTWIG, J. & FÖRSTER, E. (1997): K$\alpha_{1,2}$ and K$\beta_{1,3}$ X-ray emission lines of the 3^d transition metals. *Phys. Rev. A* **56**, 4554-4568.

JAMBOR, J.L. (1999): Nomenclature of the alunite supergroup. *Can. Mineral.* **37**, 1323-1341.

JAMBOR, J.L. & DUTRIZAC, J.E. (1983): Beaverite – plumbojarosite solid solutions. *Can. Mineral.* **21**, 101-113.

KUBISZ, J. (1970): Studies on synthetic alkali–hydronium jarosites. I. Synthesis of jarosite and natrojarosite. *Mineralogia Polonica* **1**, 47-57.

MAJZLAN, J., STEVENS, R., BOERIO-GOATES, J., WOODFIELD, B.F., NAVROTSKY, A., BURNS, P.C., CRAWFORD, M.K. & AMOS, T.G. (2004): Thermodynamic properties, low-temperature heat-capacity anomalies, and single-crystal X-ray refinement of hydronium jarosite, $(H_3O)Fe_3(SO_4)_2(OH)_6$. *Phys. Chem. Minerals* **31**, 518-531.

NIELSON, U.G., MAJZLAN, J., PHILLIPS, B., ZILIOX, M. & GREY, C.P. (2007): Characterization of defects and the local structure in natural and synthetic alunite $(K,Na,H_3O)Al_3(SO_4)_2(OH)_6$ by multi-nuclear solid-state NMR spectroscopy. *Am. Mineral.* **92**, 587-597.

NIETO, J.M., CAPITÁN, M.A., SÁEZ, R. & ALMODÓVAR, G.R. (2003): Beudantite: a natural sink for As and Pb in sulphide oxidation processes. *Trans. Inst. Mining Metall. B. Appl. Earth Sci.* **112**, 293-296.

PARKHURST, D.L. & APPELO, C.A.J. (2000): User's guide to PHREEQC (version 2) – a computer program for speciation, batch-reaction, one-dimensional transport, and inverse geochemical calculations. *U.S. Geol. Surv., Water Resources Invest. Rep.* **99–4259**.

RIPMEESTER, J.A., RATCLIFFE, C.I., DUTRIZAC, J.E. & JAMBOR, J.L. (1986): Hydronium ion in the alunite–jarosite group. *Can. Mineral.* **24**, 435-447.

ROCA, A., VIÑALS, J., ARRANZ, M. & CALERO, J. (1999): Characterization and alkaline decomposition/cyanidation of beudantite–jarosite materials from Rio-Tinto gossan ores. *Can. Metall. Quart.* **38**, 93-103.

SAVAGE, K.S., BIRD, D.K. & O'DAY, P.A. (2005): Arsenic speciation in synthetic jarosite. *Chem. Geol.* **215**, 473-498.

SCOTT, K.M. (1987): Solid solution in, and classification of, gossan-derived members of the alunite–jarosite family, northwest Queensland, Australia. *Am. Mineral.* **72**, 178-187.

SHANNON, R. (1976): Revised effective atomic radii and systematic studies of interatomic distances in halides and chalcogenides. *Acta Crystallogr.*, **A32**, 751-767.

STOFFREGEN, R.E. & ALPERS, C.N. (1987): Woodhouseite and svanbergite in hydrothermal ore deposits: products of apatite destruction during advanced argillic alteration. *Can. Mineral.* **25**, 201-211.

SZYMAŃSKI, J.T. (1985): The crystal structure of plumbojarosite $Pb[Fe_3(SO_4)_2(OH)_6]_2$. *Can. Mineral.* **23**, 659-668.

WILLS, A.S. & HARRISON, A.H. (1996): Structure and magnetism of hydronium jarosite, a model Kagomé antiferromagnet. *J. Chem. Soc. – Faraday Trans.* **92**, 2161-2166.

YOUNG, R.A. (1993): Introduction to the Rietveld method. *In* The Rietveld Method (R.A. Young, ed.). Oxford Science Publ., Oxford, U.K. (1-38).

Received December 1, 2009, revised manuscript June 1, 2010.